Dr. V. Kratky
Photogrammetric Research, Division of Physics
National Research Council of Canada
Ottawa, Ontario K1A 0R6, Canada

Real-Time Photogrammetric Support of Dynamic Three-Dimensional Control

A single camera resection combined with closed circuit video sampling techniques and digital processing hardware can be developed into a system for real-time three-dimensional control.

Introduction

P HOTOGRAMMETRY, which was originally used exclusively for cartographic purposes, gradually developed into a technique with a wider scope of applications in other technical fields, especially in engineering and biomedicine. Since photogrammetry is routinely used to monitor stationary or low-rate dynamic situations in positioning tasks, it seems to be natural to expand its use into areas in which the derived information forms a feedback to support closed-loop guidance and control systems. The difficulty is that in some instances the physical reality to be controlled is highly dynamic so that the feedback is needed with a minimum delay. Information from images must be derived quickly and processed on line before return to the feedback.

This study outlines how a real-time three-dimensional control can be achieved by combining photogrammetry, closed-circuit video sampling techniques, and dig-

KEY WORDS: **Automatic tracking; Control; Monitoring; Resection; Space shuttle orbiter; Television; Three-dimensional; Video map matching**
ABSTRACT: *An on-line photogrammetric solution using a single vidicon camera and a TV monitor was developed at the National Research Council of Canada to supply information for three-dimensional control in the close-range dynamic operation of a manipulator system, such as in the Space Shuttle Orbiter. The solution is based on a modified photogrammetric resection of the camera supported by on-line hardware providing an automatic tracking of target images in the video scan. The resection is repeatedly solved by a minicomputer within the real-time limits of the 30Hz video scanning process, with the results available for feedback in a three-dimensional control system. Geometric description of the resection and control approach is followed by an assessment of the geometric feasibility, based on computer simulations. Statistical analysis of generated data containing noise shows the effect and reliability limits of individual system components. The study indicates that a control operation can be smooth and reliable within $+5$ mm in position and a fraction of a degree in attitude. The procedure is applicable as a general tool of engineering control.*
REFERENCE: Kratky, V., "Real-Time Photogrammetric Support of Dynamic Three-Dimensional Control," *Photogrammetric Engineering and Remote Sensing,* Journal of the American Society of Photogrammetry, ASP, Vol. 45, No. AP9, September, 1979.

ital processing hardware. It is based on a project jointly undertaken at the National Research Council of Canada (NRCC) by the National Aeronautical Establishment (NAE) and the Division of Physics.

The project was to examine a potential application in the manipulation of objects in space. The examination stemmed from Canada's participation in the United States

Photogrammetric Engineering and Remote Sensing,
Vol. 45, No. 9, September 1979, pp. 1231-1242.

1231

Space Shuttle program, whereby the NAE through Canadian industry is developing the Remote Manipulator System (RMS) for the Orbiter vehicle. The Orbiter is a reusable space vehicle designed to transport a variety of payloads into Earth orbit. The payload is placed in a large cargo bay, 18.3 m long and 4.6 m in diameter, and can later be deployed or retrieved by the RMS. In order to deploy or retrieve a satellite, it is necessary to position the RMS through the operator's controls so as to place its end effector within a few centimetres of a grapple fixture on the satellite. The satellite can then be grappled and connected rigidly to the end effector and then manipulated by the operator into or out of the cargo bay. Since direct observation from the control position in the Orbiter is limited, the operation is monitored by means of TV cameras mounted on the RMS and on the Orbiter. The operator's ability to guide the end effector is thus limited by the fact that the visual presentation on the TV monitor is only in two dimensions.

There may, therefore, be a need for control of the RMS in three-dimensional space, independent of the operator's limitation of space perception. It was decided at NRCC to build on a previous experience with the single camera photogrammetric monitoring of test vehicles redirected by highway cable barriers (Kratky and van Wijk, 1971; van Wijk and Pinkney, 1972) and to demonstrate the method in real-time, using the equivalent of the Orbiter closed-circuit TV camera and on-board computer (Pinkney et al., 1976).

This study contains a geometric analysis of the photogrammetric and control tasks. Other theoretical and developmental aspects were treated by Pinkney (1978).

GEOMETRIC CONCEPTS OF THE PHOTOGRAMMETRIC APPROACH

Photogrammetric methods are capable of being used in engineering as a part of monitoring, positioning, and control systems. Because of its simplicity, a single camera resection is extremely suitable for this purpose. Even though information in a single photogrammetric picture is not sufficient to derive all three-dimensional features of a model as in stereophotogrammetry, it is still possible to determine the relative camera-object position and attitude provided that the object is a rigid body and carries a minimum of three control points. Depending on the particular application, the camera-object arrangements may differ, one of them being stable while the other is moving, or both of them moving. The

dynamic character of a situation may also require that a non-metric camera be used, e.g., a video or movie camera. Proper steps must then be taken to calibrate and correct the system for photogrammetric use.

General geometric conditions for the three-dimensional control of the RMS from information collected by a video camera are illustrated in Figure 1. The Orbiter and the satellite to be retrieved are sketched in their operational mode. They are independently moving and changing their relative position and attitude in a general, a priori unknown pattern. However, the Orbiter can be maneuvred to keep the rate of relative changes reasonably low over a needed period of time. The extended manipulator must be operated in a way to superimpose the end effector E with the satellite grappling hardware represented in Figure 1 by point G. Video camera C mounted close to E is aimed in the general direction to the satellite. In this orientation it can relay images of auxiliary control points targeted on the satellite surface.

Let us define three basic coordinate systems with origins in points O, C, and S, which are mutually rotated. Since the relative positions of pairs C-E and G-S are known, one can readily derive the six-degree-of-freedom information on the current separation E-G from monitored separation C-S determined continuously by a photogrammetric resection of the video camera from control points given in the reference system S. In order to eliminate the separation E-G as needed for a successful docking, one has to bring the camera into its final position and attitude marked by C'. From there it is aimed at point A on the satellite surface. The orientation of C' in the S-system is obviously given by the summation of the two six-component vectors S-G and E-C.

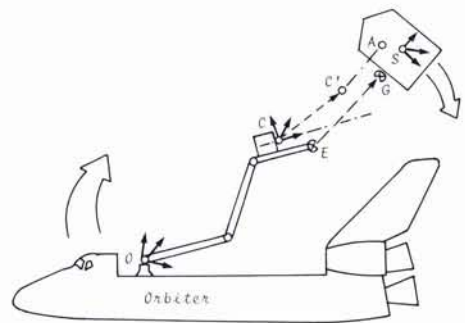The relation of O-E is mechanically con-

FIG. 1.   Function of the Remote Manipulator System.

strained by the RMS and can be servo manipulated from the Orbiter depending on the design of its components and on associated degrees of freedom. Any desired geometric translation and rotation of the end effector E must, therefore, be suitably interpreted in terms of servoed components of the RMS. This matter, as well as an analysis of other dynamic and mechanical aspects involved, are beyond the scope of a photogrammetric study and are not dealt with here. Within this study, attention is devoted to establishing the camera-object relationship (E-G or C-C') and to showing that sequentially derived information can be used reliably in a feedback to control the camera-object manoeuvre in real-time.

An individual resection is only one of a series of processes in which data input, computations, and data feedback return must be arranged in a fast cycle, the duration of which is limited by the 30 Hz video scanning process. Manual operations usually involved in photogrammetric measurements are unthinkable here, and data acquisition must be automated. In the NRCC project this has been solved by on-line hardware providing a continuous computer tracking of target images in the video scan as described by Pinkney (1978). Once identified on the TV monitor screen by an operator, the target images are locked onto by the hardware, and the on-board minicomputer will supply information on the position of the target centroids within the video scan. This position is then interpreted in terms of x', y' coordinates defined in the plane of the original optical image.

The computation proper must proceed fast enough to comply with the time limits of the video scanning process and with the capability of the on-board minicomputer, which is of the PDP-11 family. This time limitation affects both the analytical formulation of the task and the volume of control points to be used. Consequently, one should not consider a fully rigorous solution. Strictly speaking, the sequential mode of coordinate measurements is already affecting the rigor of solution and, furthermore, delays in the response of servos and inertia of the masses involved make it practically impossible to introduce corrections in the control process instantaneously, at the theoretically required time. For this reason, it is not necessary to call for an iterative refinement in the solution of non-linear relations, which is customary in stationary photogrammetric applications. The first iteration of a rigorous solution, or just a single-step approximate

solution using explicit formulas, is adequate to provide valid information for the control feedback. For a given, fixed size pattern of control points, any solution is distance-dependent and its accuracy or efficiency increases with the distance reduced. Thus, a photogrammetry-based control of a dynamic positioning operation in three dimensions is, in effect, self-refining.

SINGLE CAMERA RESECTION

Rigorous Formulation. Photogrammetric resection is applied here to determine the relative position and attitude of two moving bodies. However, for the purpose of this computation, coordinate system S of the targeted satellite control points is considered as a stable reference and computations yield six parameters for the video camera orientation within system S. A rigorous formulation is based on the well-known collinearity equations, i.e.,

$$F_x \equiv Xz - Zx = 0, \quad F_y \equiv Yz - Zy = 0. \quad (1)$$

Here X, Y, and Z are object point coordinates reduced with respect to the video camera projection center, and x, y, and z are coordinates obtained by orthogonal transformation of measured video coordinates x' and y', i.e.,

$$(x\ y\ z)^T = T\ (x'\ y'\ c)^T, \quad (2)$$

where c is calibrated principal distance (camera constant) and $T = F(\kappa, \phi, \omega)$ is a rotation matrix defining the attitude elements κ, ϕ, and ω of the camera as represented by roll, yaw, and pitch, respectively. Both coordinate systems are righthanded and the reference system is oriented with the positive Z-axis directed against the camera.

Since each control point contributes to the solution by two equations, the minimum number of control points is three. In the presence of redundant points the method of least squares is applied in its condition version represented as $Av + Bg + u = 0$. By premultiplying with A^{-1} one arrives at the parametric least squares formulation

$$-v = \bar{B} g + l, \quad \bar{B} = A^{-1}B, \quad l = A^{-1}u,$$

where A is a matrix of partial derivatives of Equations 1 with respect to measured video coordinates, B is a design matrix of the system defined with respect to the unknown orientation parameters $g^T = (X_0 Y_0 Z_0 \kappa\ \phi\ \omega)$ and u is a misclosure vector of Equations (1). Assuming that all measurements are independent and equally accurate, their weighting can be neglected. One derives the unknown parameters of orientation

$$g = -(\bar{B}^T\bar{B})^{-1}\bar{B}^Tu \qquad (3a)$$

and their variance-covariance matrix

$$Q_{gg} = (\bar{B}^T\bar{B})^{-1}. \qquad (3b)$$

Rigorous photogrammetric solutions are iteratively repeated with updated values for g, u, and possibly for $\bar{B}$, but as explained earlier, this is not needed here, since the procedure is dynamic and the update is implied in another single iteration for the following video frame. Thus, the computation retains its typical iterative character and benefits from the gradual refinement in the camera orientation. Measured video coordinates are continuously changing throughout the iterative process and are eventually stabilized when the camera is brought into its desired orientation C' within the limits of involved control components.

The computer time estimate for a single iteration of the rigorous solution is based on the speed of PDP 11/45 minicomputer requiring 6.2, 12, and 18.4 μs for addition, multiplication, and division, respectively. For the total of $(531 + 700 + 114)$ above operations the needed time reaches 14 ms which, together with additional 3 ms for fast operations, requires approximately 50 percent of the time available within the video frequency. The remaining time can be used for additional data handling, for checking, and for control computations.

Simplified Version. Because only a single iteration is applied to the solution of an individual video frame, there seems to be little merit to using a rigorous procedure in forming the matrices and in solving the normal system by time consuming matrix inversion. One can take advantage of the fact that there is a full freedom in choosing any suitable number and configuration of control points. Upon choosing a regular pattern one can easily derive an analytical form of the normal equations in which all off-diagonal elements disappear, except for those representing the well-known correlations of pairs X-ϕ and Y-ω. The unknowns can then be presolved in the analytical form and explicitly expressed as functions of original measurements. This is a known approach formulated and analyzed in various publications, e.g., by Hallert (1960) for a five-point pattern and by Goncharov (1974) for a nine-point pattern. Here, formulas are presented for the most economical configuration of four control points positioned in a plane as corners of a square figure with their coordinate origin in the center, as shown in Figure 2. This is the minimum configuration allowing for an explicit least squares solution and still yielding
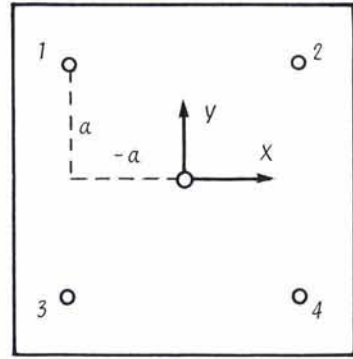

Fig. 2.   Configuration of control targets.

a redundancy of two measurements on top of six needed ones.

Because of the regular control point pattern, the absolute values of all control coordinates are the same, equal to a, and control points also define identical direction tangents $\theta = |Z/X| = |Z/Y|$. The solution of the normal equation system yields corrections for the orientation elements in an explicit form

$$dX_0 = -\frac{1}{4}\, m\, ([dx] + (\theta^2 + 1)\, [dy]_{1423}),$$

$$dY_0 = -\frac{1}{4}\, m\, ([dy] + (\theta^2 + 1)\, [dx]_{1423}),$$

$$dZ_0 = -\frac{1}{8}\, m\theta\, ([dx]_{2413} + [dy]_{1234}),$$

$$d\kappa = -\frac{1}{8}\,\frac{m}{a}\, ([dx]_{1234} + [dy]_{1324}),$$

$$d\phi = -\frac{1}{4}\,\frac{m}{a}\, \theta\, [dy]_{1423},$$

$$d\omega = -\frac{1}{4}\,\frac{m}{a}\, \theta\, [dx]_{1423}, \qquad (4)$$

where m is the scale number of the optical image and

$$[dx] = \sum_j dx_j,$$
$$[dx]_{ijkl} = dx_i + dx_j - dx_k - dx_l.$$

A stochastic evaluation of this solution yields variances of unit weight and of unknowns expressed also in an explicit analytical form (Kratky, 1978) so that they can be readily used in a computer program to estimate the degree of success in the least squares fit and the quality of derived corrections dg_i in a particular video frame.

The computer time consumption for a single frame evaluation is below 3 ms, which is only 10 percent of the time available for handling of a single video frame.

CAMERA-OBJECT CONTROL

The resection computation provides values representing an instantaneous position and attitude of the video camera in the reference system of the satellite. As shown in Figure 1 this orientation C originally differs from the desired orientation C' and the control procedure must gradually eliminate this difference. Regardless of the physical complexities, one can simplify and use a geometric analysis as a first approximation to physical solutions. This geometric assessment of control explores dynamic changes of the camera at point C, i.e., concentrates on the camera-object relationship only, and is not concerned with the control implementation in the O-E section of the system. In general, the camera is considered as an independent module manipulated in its relation to the object.

Each of the six degrees of freedom of the camera can be monitored and controlled in individual sets of sequentially derived values subjected to continuous checking and followed by hypothetical corrective actions. Each individual C'-C component is regarded as an error to be eliminated by a suitable correction in the opposite direction. Neither the camera nor the satellite are stationary, but move initially at constant velocities, different for each of the degrees of freedom. Without any control action they would gradually drift away as shown in Figure 3 (representing error e versus time t) by a straight line. A correction can obviously be applied by a suitable change of the current velocity, i.e., by a momentary negative acceleration, so eventually eliminating the components of error vector C'-C and suppressing present velocities.

Analytical Formulation. Let us consider an individual component. To generate a restoring force in the camera-object control system, the amount of correction should be dependent on the current magnitude of error e. This arrangement obviously gives rise to a harmonic motion in which error e varies sinusoidally with time. A suitable damping of this harmonic motion can be achieved by making the correction also dependent on the current error velocity $v = de/dt$. This control
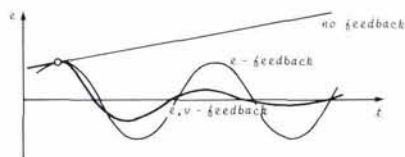

FIG. 3.   Position errors of the end effector.

component represents the effect of a resistive force in the control system. Photogrammetrically determined values of current errors e and of current velocities v are used to compute and introduce negative acceleration a which controls the errors in a damped oscillation mode.

Damped harmonic motion is analytically expressed as a function of time, i.e.,

$$e = A \exp(-kt) \cos(\omega t + \delta), \qquad (5)$$

where A is an original amplitude for an unknown time, k is a suitable coefficient to control the damping power, ω is angular frequency, and δ is phase shift. Velocity v is derived as a derivative de/dt, i.e.,

$$v = -A \exp(-kt)\{\omega\sin(\omega t + \delta) + k \cos(\omega t + \delta)\} \qquad (6)$$

and the acceleration $a = dv/dt$ is

$$a = A \exp(-kt)\{(k^2 - \omega^2) \cos(\omega t + \delta) + 2k\omega \sin(\omega t + \delta)\}. \qquad (7)$$

To accomplish the control of errors e as required by Equation 7 one must be able to define acceleration a as a function of variables e and v. By modifying Equation 7 with substitutions for the right sides of Equations 5 and 6, one derives

$$a = -(k^2 + \omega^2)e - 2kv \qquad (8)$$

which is the expected analytical form of control.

Angular frequency ω is derived from the oscillation frequency $F = 1/T$ which can be selected arbitrarily, depending on the desired period of oscillation T, i.e.,

$$\omega = 2\pi F. \qquad (9)$$

The meaning of coefficient k can then be evaluated from the selection of damping power D_p. This parameter is derived as a ratio of exponentials $\exp(-kt)$ defined for two consecutive time values separated by half of the period in the ωt-domain of oscillation. One can write

$$D_p = \exp(-kt_1)/\exp(-kt_2) = \exp(k\Delta t),$$

where

$$\Delta t = \pi/\omega = 1/2F$$

so that

$$D_p = \exp(d) = \exp(k/2F).$$

Value k is then derived as

$$k = 2dF, \qquad (10)$$

where d is a logarithmic coefficient of damping

$$d = \ln D_p.$$

Theoretical Analysis of Operator-Assisted Solution. The operator can follow the camera control operation from the TV monitor and, even though his judgement is limited to a two-dimensional space, he may attempt to participate in the computer-controlled process. As long as his actions are applied to parameters κ or Z, the interaction is possible at any time without affecting or disturbing the computer control. However, if the X, Y control is manipulated, the computer functions must be modified to eliminate the possibility of conflicting control commands. The computer program must be ready to accept the operator provided X_0, Y_0 values as constraints, to disregard correlations $X_0-\phi$ and $Y_0-\omega$, and derive values of ϕ, ω by calculating their corrections only from the corresponding diagonal elements of the normal matrix. An appropriate derivation yields formulas partly correcting for yaw and pitch, but mainly attempting to compensate for the operator's action. It seems very likely that the control procedure may become less accurate.

This can be illustrated by the accuracy analysis of the combined effect of the correlated pairs of parameters. Since the operator is not aware of yaw and pitch from his observations unless they are well pronounced, he is neglecting their presence and overriding their effect by introducing camera shifts X_0, Y_0. His operation is performed with an accuracy of camera aiming, limited by the resolution of the TV image.

In the non-assisted computer least squares solution, the combined effect of the correlated pairs of parameters ensures that the camera is eventually aimed at point A in the object (Figure 1). With the knowledge of the relevant variances and covariances one can estimate the accuracy of this 'aiming.' According to Figure 4, an error in aiming of $da = dX + Z\,d\phi$ has a stochastic model

$$Q_{aa} = Q_{XX} + 2ZQ_{X\phi} + Z^2 Q_{\phi\phi}.$$

Substitution for values Q_{XX}, $Q_{\phi\phi}$, and $Q_{X\phi}$ as derived by Kratky (1978) yields a relation
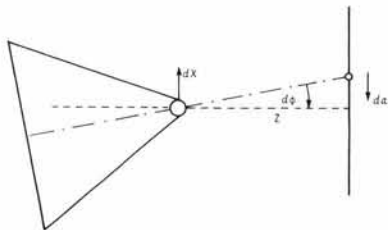

FIG. 4. Error in camera aiming.

between expected standard errors of aiming, $\hat{\sigma}_a$, and unit weight, $\hat{\sigma}_0$, of

$$\hat{\sigma}_a = \frac{m}{\sqrt{2}}\,\hat{\sigma}_0.$$

As a result of the least squares adjustment, the accuracy of camera aiming is expected to be better than the accuracy of the least squares fit and, for that matter, superior to the accuracy of individual pointing. One can conclude that the operator-assisted control of X, Y coordinates is not too useful for the control process.

OPTICAL CONSIDERATIONS

This study is based on several geometric and optical assumptions which arise from the given conditions of the mission. First, the control operation can start only after the Orbiter approaches the satellite from the appropriate direction, with minimum variations remaining in their relative orientation. To achieve this, the RMS end effector must be brought under manual control to a distance of about 3 m from the satellite grappling mechanism. Since the camera is located about 1 m back from the end effector, the operational range of the camera is between 4 and 1 m. For geometric reasons, it would be convenient to use a camera with a wide angle lens covering a field of $2\beta \simeq 90°$. This would certainly give a good stability to a single frame resection, characterized then by a factor $\theta = 1.5$. In this instance, the targeted control points should be spaced over an area framed by $2a \simeq 1.3$ m, to cover the available imaging field from the closest distance of 1 m. It is a reasonable size for a mission like Spacelab where the cylindrical body of the module is over 4 m in diameter; however, it may be too large in other instances depending on the type of mission payloads. To keep the function of the control system universal, it is realistic to settle for a shorter spacing of control points. A choice of spacing $2a$ between 0.65 and 1 m corresponds to values θ ranging from 3 to 2 and to optical fields $2\beta \simeq$ 50 to 70°.

One has to obtain a final solution meeting the expectations at the nearest distance. Both the optical and geometric performance of the camera deteriorate in the control operation in proportion to the distance, but as mentioned above the closed loop type of repeated solutions is self-refining. Its initial weakness is not at all critical if properly checked by a supporting statistical analysis during the procedure.

OPTICAL RESOLUTION AND DEPTH OF FIELD

The optical resolution of the video camera is determined by the resolution of scanning, usually given by a standard of 512 lines per frame. For a camera with focal length f and format d, the resolution element in the image plane is $\delta \simeq d/512$ and its corresponding value in the object space at the distance $h_1 = 1$ m amounts to

$$\Delta \simeq h_1 \delta / f = 1.95 \, d/f \text{ (mm)},$$

where Δ represents a minimum size of object detail resolved vertically in the video scan.

To accommodate a depth of field ranging between 1 and 4 m, the lens of the vidicon camera must use a relatively short focal length or a small aperture. With reference to Focal (1960), the near and far limits, h_1 and h_4 respectively, can be expressed as functions of hyperfocal distance H and focusing distance D

$$h_1 = \frac{HD}{H+D}, \qquad h_4 = \frac{HD}{H-D}.$$

After solving these equations for H and D, using given $h_1 = 1$ m and $h_4 = 4$ m, it follows that a camera characterized by hyperfocal distance $H = 2.67$ m and focused at $D = 1.6$ m forms a good optical image in the required range.

The hyperfocal distance should also be defined as a function of focal length f and the associated F-number $H = f^2/cF$, where c is the diameter of an acceptable confusion circle. If c is set equal to the resolution element of the video scan one can derive the appropriate F-number needed for the required depth of field, for any chosen focal length, from

$$F \geq \frac{512}{2667} \frac{f^2}{d} = 0.19 \frac{f^2}{d}. \qquad (11)$$

Table 1 gives a few examples of optical and geometrical parameters typical for the study.

GEOMETRIC CALIBRATION

Because of the limited resolution of video scanning, the lens distortion does not seem to be significant and, unless it is extremely high, it can be disregarded as a source of system inaccuracy. Also, the electronic distortion typical of TV imaging systems is less critical here than elsewhere, because image coordinates are actually determined by digital operations in the video scan referred to the optical image plane. The accuracy of derived coordinates is not affected by the quality of the final optical display on the monitor screen, which is otherwise the most critical part of video imaging systems as far as geometric distortion is concerned.

The errors inherent in the video scan usually have a pincushion character and, in a digital processing system, they can be handled by suitable polynomial expressions. Needed parameters must be derived from preflight laboratory calibration and partially checked under operational conditions by means of auxiliary fiducial or réseau marks in the optical image plane. One should keep in mind that the square pattern of chosen control points makes the effect of video distortions on the resection less critical than for a general configuration. The self-refining feature of the dynamic control procedure helps to disregard a certain level of errors during the operation as well. In laboratory experiments with the on-line video scanning processor the geometric stability of a non-corrected video scan was maintained within 5 μm in the vidicon image plane (Pinkney, 1978).

At present it is intended to extend experiments into procedures employing a self-calibration principle with tilted two-dimensional grids, after the position of the principal point is derived in a separate procedure. Future experiments will also include calibration tests of a zoom lens which could help to make the resection accuracy less dependent on the distance. With the zoom lens, the image scale can be kept con-

TABLE 1. OPTICAL AND GEOMETRIC CONDITIONS

Focal length	Format size	Control separation	Maximum video coord's	Maximum direct. tangent	Resolved video element	Resolved object element	Scale factor	Required F-number
f mm	d mm	$2a$ m	a' mm	ϑ	δ μm	Δ mm	m	F
20	25	1.00	10	0.50	50	2.5	50x	>3
20	25	0.67	7	0.33	50	2.5	50x	>3
50	40	0.67	17	0.33	78	1.5	19x	>12

stant by utilizing the full size of the video camera format.

Tests of Geometric Feasibility

geometric simulation of camera-object control

A certain advantage of technical operations in outer space is that the number of unpredictable physical factors and associated irregularities affecting operations is limited. The rules of mechanics govern with little interference so that individual objects preserve their inertia in all six degrees of freedom by moving uniformly and at constant speeds. The camera-object relationship and control can be simulated by computer. Thus, relevant dynamic procedures can be monitored in real-time and their simplified mathematical and stochastic models can be studied.

Our computer simulation of the camera control is based on an arbitrarily chosen initial camera orientation described by six values for the position and attitude of camera and by six other values corresponding to their respective velocities. This chosen orientation is considered as *real* for the purpose of simulations and is represented by C in Figure 5. From the orientation parameters and from the coordinates of control points on the satellite, fictitious video coordinates are computed by using rigorous formulas of a central projection. These coordinates are then used in the approximate resection solution yielding *computed* orientation elements represented by $\bar{C}$ in Figure 5. These computed elements may be close to, but not identical with, the real ones. The computation of video coordinates and of derived orientation elements represents a single iterative step describing the current status at a given time which is also monitored by computer. The computed elements are compared with elements of the *wanted* final orientation (marked as C' in Figure 5) and the differences are considered as current
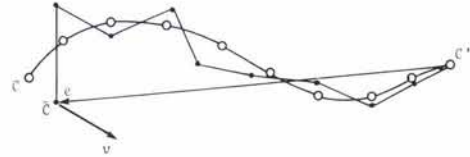

FIG. 5.   Geometry of the control approach.

control errors e. In order to simulate the control loop, one also needs current relative velocities, but these can be determined only after several iterative steps. As long as their contribution in the control loop is disregarded, the control procedure generates an undamped harmonic motion of the guided camera. Corrective acceleration as computed from Equation 8 is now applied to change current real velocities, and the whole cycle is repeated in the next step started with the generation of new video coordinates. The time history of the simulation is sketched in Figure 6. The real orientation is repeatedly updated, at the beginning of a new cycle and at the time of the control action, from current real velocities and elapsed time intervals. The response time of the control system is disregarded in our geometric simulation.

The computation of velocities from two consecutive iterations was found inadequate because of the high noise in computed values. The interval must be stretched over six to ten iterations to yield acceptable results and even then the inaccuracy can occasionally be too high. All computed values e and v are continuously checked by comparing them with values from the previous iteration. Since the control procedure does not allow for any abrupt changes, the difference should statistically comply with estimates of standard errors computed in each iteration. If a specified confidence interval is exceeded, the computer element is considered unreliable and the corresponding control correction is disregarded in the current iteration. The simulation is also controlled by
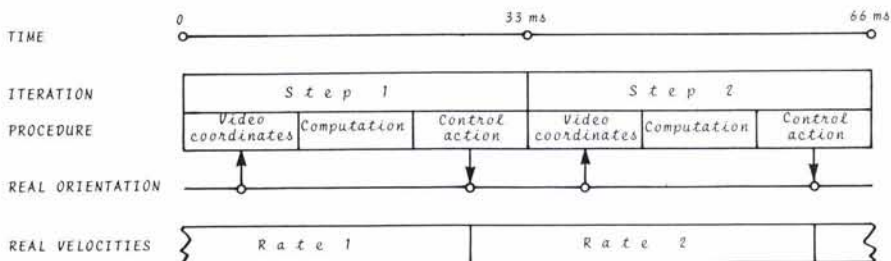

FIG. 6.   Time history of control simulations.

specified upper limits for acceleration pulses applied in the control and for acceptable velocities of orientation elements. All these safeguards change slightly the character of the resulting control motion and contribute to its slower convergence. The iterative process is then run until all simulated errors e and v comply with specified tolerances.

The simulation program is universal in allowing for different geometric and optical conditions, and for an arbitrary initial orientation. Also entered as input are coefficients k and ω controlling the damping power and desired period of oscillation, respectively. The most useful feature of the program, however, is its ability to generate random errors representing noise or functional inaccuracies in various components of the control system. Their effect can then be followed throughout the procedure. In this way, the geometric feasibility of the photogrammetric approach and its reliability can be thoroughly tested. Of particular interest is a simulation of the system response to the increased noise in input video coordinates, because this helps to specify required levels of the basic video resolution and calibration.

All information collected during a simulation run is stored and subsequently printed out for further analysis of details and for a numerical documentation of any particular aspect studied. For a fast interpretation and better visualization of the control procedure, the real orientation elements are also displayed in a crude graphical form using a lineprinter. Figure 7 contains an example of such a print. The situation in each iteration is displayed in a single line by symbols X, Y, Z, $K(\kappa)$, $P(\phi)$, and $O(\omega)$ for the orientation elements. Because of the limited print resolution, the horizontal scale is reduced ten times whenever a value exceeds the width of the graph, e.g., parameter O in the 10th and 11th iterations. The spacing between vertical bars corresponds to 100 or 10 mm for positional elements and to 100 or 10 mrad for attitude elements.

Numerous tests were run with the simulator in an effort to obtain better insights into the basic geometric function of the control system. Simulations were also very useful in stochastic modeling of relations needed for a statistical analysis of large samples of data. Examples of the most typical tests are presented in the following section. To make comparisons possible, the examples are based on the same pattern of initial orientation, assuming the use of a video camera with $f = 53$ mm, $d = 40$ mm, θ
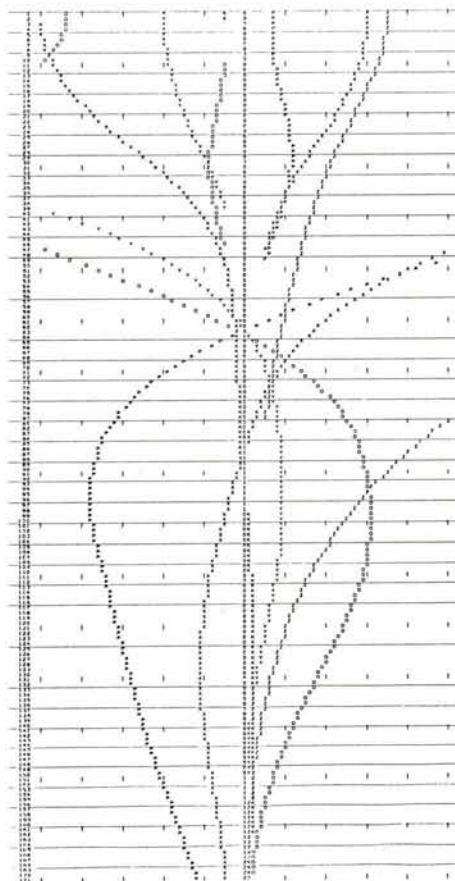

FIG. 7. Graphical representation of simulated control.

$= 3$, and with the nominal resolution element in the image plane $\delta = 78$ μm. Factor ω is defined for a low frequency of oscillation, $F = 0.1$, and is also kept unchanged throughout the examples.

CONVERGENCE OF THE PROCESS

Our simulations generate basically two sets of data representing sequences C, $\bar{C}$ of real and computed elements, respectively. As shown in Figure 5, the C-sequence is rather smooth while the other is discontinuous. However, in most instances both sequences eventually converge towards C' and stay close within 5 mm for positions or 5 mrad for attitude elements. Relative velocities are successfully kept below 30 mm/s or 30 mrad/s.

The convergence of the process indirectly serves also as a general indicator of its accuracy. If the individual computed values are not sufficiently accurate the control efficiency is lowered and it takes longer to bring

errors e below given tolerances. The absolute number of needed iterations increases with the standard error σ_x in video coordinates as follows:

σ_x	0	30	50	100	150	μm
iterations	192	203	218	425	850	$\times$

An analysis of data from auxiliary printouts shows that the convergence deteriorates because sequences C of computed elements are becoming increasingly noisy with increased σ_x. However, the control is still efficient and reliable up to the level of $\sigma_x = 100$ μm. Beyond this limit the procedure becomes erratic. The residual oscillation is too pronounced and the above mentioned tolerances may not be met easily; they should then be relaxed.

A similar test conducted with an increased power of damping $D_\mu = 150$, yields

σ_x	0	50	100	150	μm
iterations	138	142	397	∞	$\times$

As one would expect, the rate of convergence was improved, but again, the process is not controllable beyond $\sigma_x = 100$ μm, unless the tolerances are relaxed. Figure 8 shows parts of the graphical representations for both extreme cases of this test and demonstrates the difference between a smooth and erratic response of the system.

In both previous examples relative velocities were computed from two extreme values over six iteration steps. Considering the noisy character of data this is a rather crude mode of operation. A significant improvement is achieved if the velocities are

computed over the same interval of six values, but with the use of a linear fit to all available data. Using a damping coefficient $D_\mu = 100$ which is also applied in all following examples, the convergence rate becomes less dependent on σ_x as demonstrated by

σ_x	0	50	100	μm
iterations	235	250	273	$\times$

In the following tests the conditions of simulation were unchanged, but the computer control was modified to consider a suitable *aiming* of the camera as an additional factor. Instead of steadily comparing computed yaw ϕ and pitch ω with the wanted zero values eventually expected to result from the control procedure, yaw and pitch were controlled to aim the camera in the direction of object point A (Figure 1) by means of an additional constraint in the computation. This procedure simulates the assisting function of the operator as discussed earlier. The convergence of the process was significantly slower as demonstrated by the sharply increased number of iterations in tests based on $s_x \neq 0$

σ_x	0	50	100	μm
iterations	270	410	639	$\times$

Furthermore, X_0 and Y_0 components became less stable and subjected to unexpected random variations. This experience is in agreement with the above theoretical analysis finding the operator-assisted control to be less efficient.

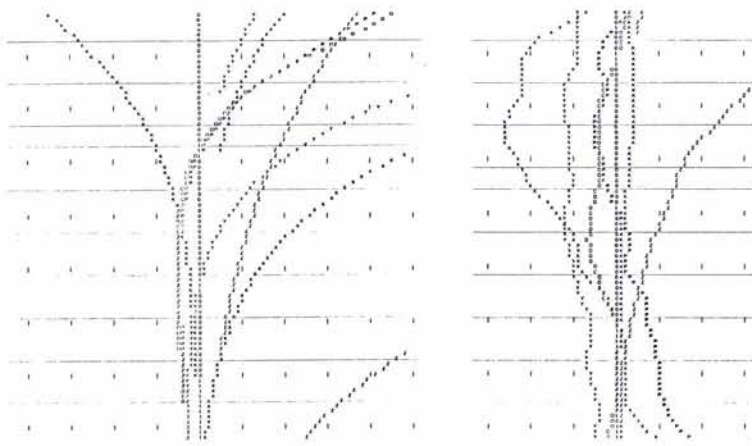The idea of the operator-assisted control

FIG. 8.   Effect of errors in the video input.

was further tested in special simulations aided by an auxiliary CRT display used on line with the computer. The procedure of aiming during the control process was simulated by graphically generating a simplified version of what can be observed on the TV monitor. In numerous experiments it was repeatedly confirmed that the control procedure is not improved by this additional constraint. The convergence of control invariably deteriorated in instances when the operator assisted in the computer simulated control solution.

STATISTICAL ANALYSIS OF SIMULATED EXPERIMENTS

Equations 4 used in single control iterations are not rigorous and their inaccuracy is proportional to the magnitude of computed values e in the control loop. The inaccuracy results from neglect of higher order terms in the expansion of formulas and also depends on the current geometrical configuration, as represented by values h, a, and f. This lack of rigor is one of the major error sources in the control process. Nevertheless, the magnitude of values e is gradually reduced throughout the process and, thus, the accuracy of the non-rigorous formulas is improved as well. This fact reflects the effect of refinement which is inherent to iterative solutions. Another major error source is represented by the accuracy limits of input video coordinates. On approaching the point of grappling, this source is also becoming less critical because of the improved geometric configuration for the solution.

Both error sources were statistically tested by means of computer modeling of the stochastic relations involved. A generator of random numbers with a normal distribution produced values at the level of dispersion of σ_p^2 to represent the uncertainty in the current camera orientation, and also generated values characterized by variance σ_x^2 representing the noise in video coordinates. Tests were arranged for different combinations of σ_p and σ_x with computations repeated 100 or 200 times for each case. Repeatedly generated were orientation parameters C distorted by σ_p, and video coordinates x' and y' distorted by σ_x. Computed orientation was derived in two versions from either undistorted or distorted video coordinates, respectively. A statistical analysis of differences between the two versions yielded estimates of solution errors due to inaccurate formulas and of solution errors due to inaccurate video coordinates.

It has been found and reported in more detail by Kratky (1978) that the effect of the approximate formulation upon computed elements is compounded by the magnitude of σ_p, but is independent of σ_x. In turn, the effect of errors in input video coordinates was proven to be independent of σ_p. The figures derived in the simulations are in complete agreement with analytical formulations of expected variances of derived orientation parameters, and all of them can be described as h-dependent. Standard errors σ_{X_0}, σ_{Y_0} are proportional to h^3, whereas standard errors σ_{Z_0}, σ_ϕ, σ_ω are proportional to h^2 and standard error σ_κ is proportional to h. In all stochastic tests conducted, the standard error of unit weight was found to be identical with σ_x, which confirms the expected identity of a priori and a posteriori estimates.

CONCLUSIONS

A current NRCC project demonstrated that a photogrammetric single camera resection combined with closed circuit video sampling techniques and digital processing hardware can be developed into a system for real-time three-dimensional control. The system can be implemented in engineering as an object sensing and following device or, in a modular form, as a position and velocity transducer. In space applications, such as in the Space Shuttle program, the system may serve to manipulate payloads under automatic remote control. In this study, an analysis of associated photogrammetric and control formulations, supported by simplified computer simulations, proved the *geometric* feasibility of the proposed closed loop system. The techniques have a general potential and are believed to have widespread applications in several other dynamic engineering tasks where the real time aspect is crucial to the operation. These may be, for instance, remote control and manipulation of objects in nuclear laboratories and power plants, special technical operations performed underwater, machine position and orientation tasks, automatic docking of supertankers, etc.

REFERENCES

Focal, 1960. *The Focal Encyclopedia of Photography*, Focal Press Ltd., London.

Goncharov, A. P., 1974. Solution Accuracy for Photogrammetric Resection of a Single Photograph (in Russian), *Trudy CNIIGAiK*, Vol. 33.

Hallert, B., 1960. *Photogrammetry*, McGraw-Hill, New York.

Kratky, V., and M. C. van Wijk, 1971. Photogrammetry Used to Determine the Motion of a Vehicle Crashing into a Highway Barrier, *Bulletine de la Société Francaise de Photogrammétrie*, No. 42.

Kratky, V., 1978. Analytical Study of a Photogrammetric Solution for Real-Time Three-Dimensional Control, *Proceedings of the ISP Symposium on Photogrammetry for Industry*, August 1978, Stockholm.

Pinkney, H. F. L., C. I. Perratt, V. Kratky, and A. A. Ayad, 1976. *On the Application of Automatic, Real-Time Single Camera Photogrammetry to Derive the Relative Spatial Orientation and Position of Objects in Machine Tasks.* A Conceptual Outline and Preliminary Evaluation, NRCC, NAE Internal Report, Feb. 1976. For reference purposes: NRCC, NAE Laboratory Technical Report LTR-ST-1007.

Pinkney, H. F. L., 1978. Theory and Development of an On-Line 30 Hz Video Photogrammetry System for Real-Time Three-Dimensional Control, *Proceedings of the ISP Symposium on Photogrammetry for Industry*, Aug. 1978, Stockholm.

van Wijk, M. C., and H. F. L. Pinkney, 1972. A Single Camera Method for the 6-Degree of Freedom Sprung Mass Response of Vehicles Redirected by Cable Barriers, *Proceedings of the SPIE Seminar on Optical Instrumentation—A Problem Solving Tool in Automotive Safety*, Nov. 1972, Detroit.

Notice to Contributors

1. Manuscripts should be typed, double-spaced on 8½ × 11 or 8 × 10½ white bond, on *one* side only. References, footnotes, captions—everything should be double-spaced. Margins should be 1½ inches.
2. Ordinarily *two* copies of the manuscript and two sets of illustrations should be submitted where the second set of illustrations need not be prime quality; EXCEPT that *five* copies of papers on Remote Sensing and Photointerpretation are needed, all with prime quality illustrations to facilitate the review process.
3. Each article should include an abstract, which is a *digest* of the article. An abstract should be 100 to 150 words in length.
4. Tables should be designed to fit into a width no more than five inches.
5. Illustrations should not be more than twice the final size: *glossy* prints of photos should be submitted. Lettering should be neat, and designed for the reduction anticipated. Please include a separate list of captions.
6. Formulas should be expressed as simply as possible, keeping in mind the difficulties and limitations encountered in setting type.

Journal Staff